Iterative Sparse Channel Estimation and Decoding for Underwater MIMO-OFDM

Jie Huang, Jianzhong Huang, Christian R. Berger, Shengli Zhou, and Peter Willett
Department of Electrical and Computer Engineering, University of Connecticut, Storrs, CT 06269, USA

***Abstract*— In this paper we propose a block-by-block iterative receiver for underwater MIMO-OFDM that couples channel estimation with MIMO detection and channel decoding. In particular, the channel estimator is based on a compressive sensing technique to exploit the channel sparsity, the MIMO detector consists of a hybrid use of successive interference cancellation and soft MMSE equalization, and the channel codes used are nonbinary LDPC codes. Various feedback strategies such as hard, soft, and thresholded symbol feedback are studied. We test the receiver performance using simulation and experimental data collected from the RACE08 and SPACE08 experiments. All iterative receivers show impressive gains over a non-iterative receiver.**

I. Introduction

Multi-input multi-output (MIMO) techniques have been recently applied in underwater acoustic systems to drastically improve the spectrum efficiency. Experimental results have been reported in [1]–[9] for single carrier systems, and in [6], [10]–[15] for multicarrier systems, in the form of orthogonal frequency division multiplex (OFDM).

In this paper, we deal with MIMO-OFDM in underwater acoustic (UWA) channels. A block-by-block receiver was developed in [10], where Maximum A Posteriori (MAP) and zero forcing (ZF) detectors are used for MIMO demodulation following least-squares (LS) based channel estimation. Receivers for both spatial multiplexing and differential space time coding have been developed in [11]. Adaptive MIMO detectors have been proposed in [13], [14], where channel estimates based on the previous data block are used for demodulation of the current block after combined with phase tracking. All the receivers in [10], [11], [13], [14] are non-iterative. In [12], an iterative receiver has been presented for MIMO-OFDM that iterates between MIMO demodulation and channel decoding.

In this paper, we propose an iterative receiver that couples channel estimation, MIMO demodulation and channel decoding. The differences from [12] are the following:

1) Channel estimation is included in the iteration loop so that refined channel estimates become available along the iterations.
2) The LS channel estimator is replaced by a more advanced channel estimator recently tested in [16], [17], that exploits the sparse nature of UWA channels.

When channel estimation is included in the iteration loop, data symbols estimated in the previous round can be utilized as additional pilots to improve the channel estimation accuracy. We investigate different feedback strategies, including hard and soft feedback, as well as a novel approach based on thresholded symbol estimates. We compare the performance using numerical simulation and experimental data collected from the RACE08 and SPACE08 experiments. Iterative receivers outperform a non-iterative receiver considerably.

Note that iterative channel estimation and decoding has been heavily investigated in the literature of wireless radio communication. For example, references [18]–[20] considered different hard and soft feedback strategies with pilot symbol assisted modulation (PSAM) over time-selective flat-fading channels. Reference [21] considered cross-entropy based feedback. Specifically to underwater acoustic communication, iterative channel estimation and decoding has been studied and tested with real data in [22], where only single transmitter OFDM and hard decision feedback are considered.

The rest of this paper is organized as follows. Section II introduces the system model. Section III presents the details on the iterative receiver. Simulation results are reported in Section IV. Experimental results are reported in Sections V and VI with data collected in RACE08 and SPACE08 experiments, respectively. We conclude in Section VII.

II. System Model

A. MIMO-OFDM Transmission

We use zero-padded (ZP) OFDM. Let T denote the OFDM symbol duration and T_g the guard interval for the ZP. The total OFDM block duration is $T' = T + T_g$ and the subcarrier spacing is $1/T$. The kth subcarrier is at frequency

$$f_k = f_c + k/T, \quad k = -K/2, \ldots, K/2 - 1, \tag{1}$$

where f_c is the carrier frequency and K subcarriers are used so that the bandwidth is $B = K/T$.

For a MIMO-OFDM system with N_t transmitters, we use spatial multiplexing to transmit N_t parallel data streams. Specifically, within each OFDM block, N_t independent bit streams are separately encoded with a nonbinary low-density parity-check (LDPC) code [23]. Let $s_\mu[k]$ denote the encoded information symbols, e.g., QPSK or QAM, to be transmitted on the kth subcarrier by the μth transmitter. The non-overlapping sets of active subcarriers $\mathcal{S}_A$ and null subcarriers $\mathcal{S}_N$ satisfy $\mathcal{S}_A \cup \mathcal{S}_N = \{-K/2, \ldots, K/2 - 1\}$; the null subcarriers are used to facilitate Doppler compensation at the

This work is supported by the NSF grant CNS-0721834, the ONR grants N00014-07-1-0805 (YIP) and N00014-09-1-0704 (PECASE).

receiver [24]. The signal transmitted by the μth transmitter is given by

$$\tilde{x}_\mu(t) = \mathrm{Re}\left\{ \left[\sum_{k\in\mathcal{S}_\mathrm{A}} s_\mu[k] e^{j2\pi \frac{k}{T} t} q(t) \right] e^{j2\pi f_c t} \right\}, \quad t \in [0, T+T_g], \quad (2)$$

where $q(t)$ describes the zero-padding operation, i.e.,

$$q(t) = \begin{cases} 1 & t \in [0, T], \\ 0 & \text{otherwise.} \end{cases} \quad (3)$$

Accounting for all the overheads due to guard interval, channel coding, pilot, and null subcarriers, the overall spectral efficiency in terms of bits per second per Hz (bits/s/Hz) is:

$$\alpha = N_t \frac{T}{T+T_g} \frac{|\mathcal{S}_D|}{K} \cdot r_c \log_2 M, \quad (4)$$

where r_c is the code rate, M is the constellation size and $\mathcal{S}_D \subset \mathcal{S}_A$ is the set of data subcarriers (excluding pilot tones). With a bandwidth B, the data rate is $R = \alpha B$ bits per second.

B. Receiver Preprocessing

The same receiver preprocessing as in [12] will be applied. The received signal could be resampled to compensate a dominant Doppler effect if necessary. After resampling each receiver assumes one common Doppler shift on all transmitted data streams, and uses the energy on the null subcarriers as an objective function to search for the best Doppler shift estimate [12]. Doppler shift compensation is done at each receiver separately.

Let $z_\nu[k]$ denote the output on the kth subchannel at the νth receiver, performing ZP-OFDM demodulation on the received block after Doppler compensation. As in [12], we will use the following channel input-output model

$$z_\nu[k] = \sum_{\mu=1}^{N_t} \tilde{H}_{\nu,\mu}[k] s_\mu[k] + n_\nu[k], \quad (5)$$

where $\tilde{H}_{\nu,\mu}[k]$ is the frequency response between the μth transmitter and the νth receiver at the kth subcarrier, and $n_\nu[k]$ is the additive noise at the demodulator output, which includes both the ambient noise and the residual intercarrier interference (ICI).

III. Iterative Sparse Channel Estimation and Decoding

The proposed iterative receiver processing with N_t transmitters and N_r receivers is shown in Fig. 1, where the dotted line represents feedback from the LDPC decoder. We next specify the key modules in the iteration loop: sparse channel estimation, MIMO detection, and channel decoding.

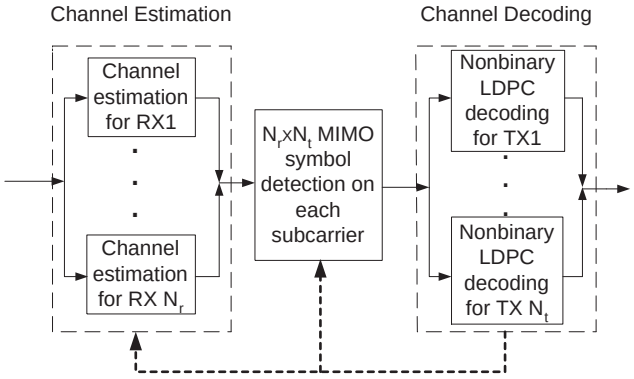

Fig. 1. Iterative channel estimation and decoding for MIMO-OFDM

A. Sparse Channel Estimation

For each transmitter-receiver pair, we assume a baseband channel with N_p distinct paths, with each path characterized by a complex amplitude ζ_p and a delay τ_p, (c.f. [16], [17]):

$$h(t) = \sum_{p=1}^{N_p} \zeta_p \delta(t - \tau_p), \quad (6)$$

such that

$$\tilde{H}[k] = \sum_{p=1}^{N_p} \zeta_p e^{-j2\pi k \frac{\tau_p}{T}}, \quad (7)$$

where we omit the transmitter and receiver index for compact notation.

Define $\tilde{\mathbf{h}}$ and $\mathbf{w}(\tau_p)$ as column vectors containing $\tilde{H}[k]$ and $e^{-j2\pi k \frac{\tau_p}{T}}$ across subcarriers, we have

$$\tilde{\mathbf{h}} = \sum_{p=1}^{N_p} \zeta_p \mathbf{w}(\tau_p). \quad (8)$$

1) Overcomplete Delay Dictionary: To formulate the compressed sensing problem, we need to use a large, but finite, dictionary. We consider a set of uniformly spaced delays as,

$$\tau_p \in \left\{ \frac{T}{\beta K}, \frac{2T}{\beta K}, \ldots, T_g \right\}, \quad (9)$$

which will lead to a dictionary of $N_\tau = \beta K T_g / T$ entries. Note that the delay spacing is chosen as a fraction of the baseband sampling interval T/K, where β is the oversampling factor. With this we construct a matrix as

$$\mathbf{W} = \left[\mathbf{w}\left(\tfrac{T}{\beta K}\right) \quad \mathbf{w}\left(\tfrac{2T}{\beta K}\right) \quad \cdots \quad \mathbf{w}\left(T_g\right) \right], \quad (10)$$

and rewrite (8) as

$$\tilde{\mathbf{h}} = \mathbf{W}\boldsymbol{\zeta}, \quad (11)$$

where $\boldsymbol{\zeta}$ contains the N_τ possible delays corresponding to the dictionary columns but should be sparse with a limited number of nonzero entries.

Now, we include the transmitter and receiver indexes, and define $\mathbf{z}_\nu$, $\mathbf{s}_\mu$, and $\mathbf{n}_\nu$ as column vectors that contain the $z_\nu[k]$,

$s_\mu[k]$, and $n_\nu[k]$ for all subcarriers containing known symbols (either pilots or symbol estimates from the LDPC decoder). We then have

$$\mathbf{z}_\nu = \sum_{\mu=1}^{N_t} [\mathbf{D}_{\mathbf{s}_\mu}\mathbf{W}]\boldsymbol{\zeta}_{\nu,\mu} + \mathbf{n}_\nu, \tag{12}$$

where $\mathbf{D}_{\mathbf{s}_\mu}$ is a diagonal matrix with the elements of vector $\mathbf{s}_\mu$ on its main diagonal, and $\boldsymbol{\zeta}_{\nu,\mu}$ contains the N_τ possible delays corresponding to the dictionary columns for the channel from the μth transmitter to the νth receiver.

For a more compact notation, define

$$\boldsymbol{\Psi} = \left[\mathbf{D}_{\mathbf{s}_1}\mathbf{W}, \quad \mathbf{D}_{\mathbf{s}_2}\mathbf{W}, \quad \cdots, \quad \mathbf{D}_{\mathbf{s}_{\mathrm{N_t}}}\mathbf{W}\right], \tag{13}$$

$$\boldsymbol{\zeta}_\nu = \left[\boldsymbol{\zeta}_{\nu,1}^T, \quad \boldsymbol{\zeta}_{\nu,2}^T, \quad \cdots, \quad \boldsymbol{\zeta}_{\nu,N_t}^T\right]^T, \tag{14}$$

where $(\cdot)^T$ stands for transpose. We then rewrite (12) as

$$\mathbf{z}_\nu = \boldsymbol{\Psi}\boldsymbol{\zeta}_\nu + \mathbf{n}_\nu \tag{15}$$

that depends on the pilots and known symbol estimates $s_\mu[k]$ via the matrix $\boldsymbol{\Psi}$.

2) Basis Pursuit Formulation: Sparse channel estimation can be formulated as a convex optimization problem using what is commonly referred to as l_1-regularization. This approach is called Basis Pursuit (BP), see e.g., [25], [26]. Specifically, BP seeks the solution of

$$\min_{\boldsymbol{\zeta}_\nu} |\mathbf{z}_\nu - \boldsymbol{\Psi}\boldsymbol{\zeta}_\nu|^2 + \lambda|\boldsymbol{\zeta}_\nu|_1, \tag{16}$$

where the parameter λ controls the sparsity of the solution $\boldsymbol{\zeta}_\nu$. Note that for a complex vector $\boldsymbol{\zeta}$, its l_1-norm is defined as:

$$|\boldsymbol{\zeta}|_1 = \sum_{n=1}^{N_t N_\tau} \sqrt{|\mathrm{Re}(\zeta_n)|^2 + |\mathrm{Im}(\zeta_n)|^2}. \tag{17}$$

An efficient implementation for the complex valued version of BP has been suggested in the appendix of [26].

B. MIMO Detection

After the path weights and delays have been estimated, frequency response at data subcarriers can be calculated using (7). At each subcarrier, we stack the received data from N_r receiving-elements [c.f. (5)] as

$$\mathbf{z}[k] = \begin{bmatrix} z_1[k] & \cdots & z_{N_r}[k] \end{bmatrix}^T. \tag{18}$$

Let $\tilde{\mathbf{H}}[k]$ denote the $N_r \times N_t$ channel matrix with the (ν,μ)-element as $\tilde{H}_{\nu,\mu}[k]$, and let $\mathbf{s}[k]$ contain N_t transmitted symbols on the k-th subcarrier. The matrix-vector channel model for each subcarrier is

$$\mathbf{z}[k] = \tilde{\mathbf{H}}[k]\mathbf{s}[k] + \mathbf{n}[k], \tag{19}$$

where $\mathbf{n}[k]$ is the additive noise. We assume that the noise on different receivers is uncorrelated and Gaussian distributed.

To demodulate $\mathbf{s}[k]$ from (19), we use the MIMO detector of [12] which consists of a hybrid use of successive interference cancellation and soft MMSE demodulation; see [12] for details.

C. Nonbinary LDPC Decoding and Feedback Information

With the outputs from the MMSE equalizer, nonbinary LDPC decoding as in [23] is run separately for each data stream. The decoder outputs the decoded information symbols and the updated posterior probabilities, which are used in the next iteration of channel estimation and equalization. During the decoding process, if all the parity check conditions of one data stream are satisfied, the decoder will declare successful recovery of this data stream. In this case we will assume that all symbols of this data stream are known without uncertainty.

To use feedback in channel estimation or MIMO demodulation, we need estimates of the unknown data $\hat{s}_\mu[k]$ and a measure of the uncertainty left in these estimates. Based on the previous round of decoding, the LDPC decoder will output posterior probabilities for each symbol, as well as probabilities based on extrinsic information only. While the extrinsic information is used in the MIMO demodulation [12], the posterior probabilities will be used to improve channel estimation:

$$\Pr\left(s_\mu[k] = \alpha_m\right), \quad m = 1, \ldots, M \tag{20}$$

where the α_m are the constellation symbols.

There are three main feedback strategies in the literature (see [18]–[20]), varying by the definition of $\hat{s}_\mu[k]$:

1) Full soft feedback

$$\hat{s}_\mu^{(s)}[k] = \sum_{m=1}^{M} \Pr\left(s_\mu[k] = \alpha_m\right)\alpha_m$$

2) Full hard feedback

$$\hat{s}_\mu^{(h)}[k] = \alpha_{m^*}, \quad m^* = \arg\max_m \Pr\left(s_\mu[k] = \alpha_m\right)$$

3) Threshold controlled hard feedback

$$\hat{s}_\mu^{(th)}[k] = \begin{cases} \hat{s}_\mu^{(h)}[k], & H(s_\mu[k]) < \Gamma_h \\ 0, & \text{otherwise,} \end{cases}$$

where $H(s_\mu[k])$ stands for the entropy. In other words, only when the symbol estimate is viewed as reliable enough, a hard decision is made for feedback.

A novel strategy we consider is based on thresholding the soft feedback, i.e., only soft feedback symbols whose absolute value is larger than a threshold will be used.

$$\hat{s}_\mu^{(ts)}[k] = \begin{cases} \hat{s}_\mu^{(s)}[k], & \left|\hat{s}_\mu^{(s)}[k]\right| > \Gamma \\ 0, & \text{otherwise.} \end{cases}$$

For a constellation with non-constant modulus, such as 16-QAM, symbols of larger amplitude are more likely to be included into feedback for channel estimation.

IV. Numerical Simulation

We use an OFDM system with the following specifications: carrier frequency $f_c = 13$ kHz, $K = 1024$ subcarriers, symbol duration $T = 104.86$ ms, and the guard time is $T_g = 24.6$ ms. The bandwidth is then $B = 9.7656$ kHz. There are $|\mathcal{S}_P| = K/4 = 256$ pilot tones and $|\mathcal{S}_N| = 96$

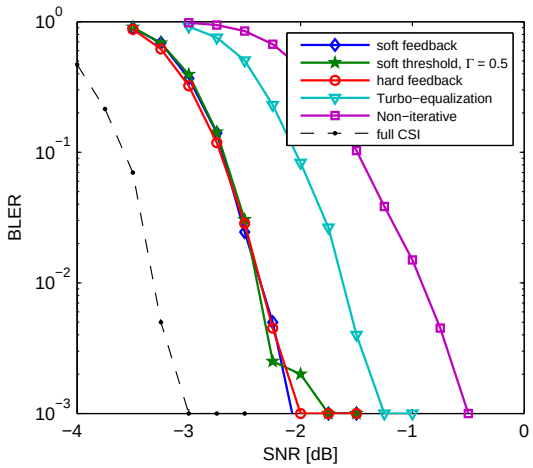

Fig. 2. Simulation results for MIMO-OFDM, $N_t = 2$, $N_r = 4$, QPSK

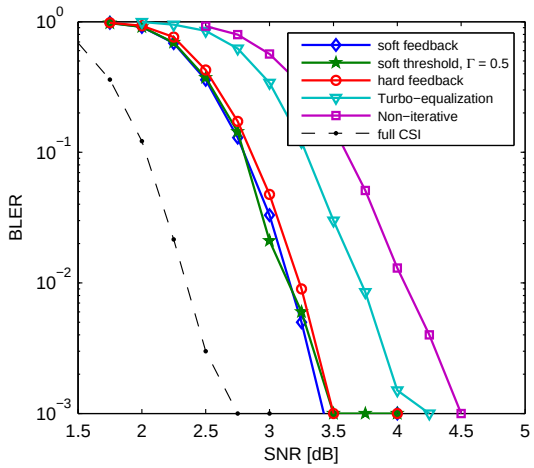

Fig. 3. Simulation results for MIMO-OFDM, $N_t = 2$, $N_r = 4$, 16-QAM

Null subcarriers for edge protection and Doppler estimation, leaving $|\mathcal{S}_D| = 672$ data subcarriers. The data within each OFDM symbol is encoded using a rate $1/2$ LDPC code from [23], and modulated using either QPSK or 16-QAM.

We consider a MIMO system with $N_t = 2$ transmitters. The data rates are 10.4 kb/s and 20.8 kb/s for QPSK and 16-QAM modulations, respectively. The 256 pilots are divided into non-overlapping sets for the transmitters where each transmitter has the same number of pilots. The pilot patterns are randomly drawn, rendering irregular positioning [12].

For the simulation scenario we generate $N_p = 15$ discrete paths, where the inter-arrival times are exponentially distributed with mean of 1 ms. The amplitudes of each path are Rayleigh distributed, with decreasing mean as the delay increases. As each OFDM symbol is encoded separately, we will use block-error-rate (BLER) as figure of merit. In the simulation each OFDM symbol experiences an independently generated channel. The pilot symbols are drawn from the QPSK constellation whereas the data symbols are drawn from QPSK or 16-QAM constellations. The pilots are scaled to ensure that about one third of the total transmission power is dedicated to channel estimation independent of the number of transmitters. We simulate the BLER performance at different SNR levels, where SNR is the signal to noise power ratio on the data subcarriers.

In Figs. 2 and 3, we compare different receivers for a MIMO-OFDM system where $N_t = 2$ and $N_r = 4$.

- "*Non-iterative*" receiver as in [10], but with the LS channel estimator replaced by the BP estimator.
- "*Turbo-equalization*" receiver as in [12], but with the LS channel estimator replaced by the BP estimator.
- The proposed iterative receiver with "*soft feedback*" with or without thresholding.
- The proposed iterative receiver with full "*hard feedback*"[1].

[1]In all subsequent figures, "Non-iterative", "Turbo-equalization", "soft feedback", and "hard feedback" are used as legends for different receivers.

Also we include a case with full channel state information (CSI), that still iterates between MIMO demodulation and LDPC decoding, but has a perfect channel estimate.

Figs. 2 and 3 show that, in this setting, employing an turbo equalization receiver gains between 0.5 and 1 dB over a non-iterative receiver, while including channel estimation in the iteration loop gains 0.5 dB. There is a gap of about 1 dB of the proposed receiver in comparison to the full CSI case.

V. Experimental Results: RACE08

The RACE08 experiment was held in the Narragansett Bay, Rhode Island, in March 2008. The water depth in the area is between 9 and 14 meters. The system parameters are the same as in the numerical simulation, except for a different bandwidth of $B = 4.88$ kHz. The corresponding symbol duration and subcarrier spacing are $T = K/B = 209.7$ ms and $1/T = 4.8$ Hz, respectively.

We will focus on three days of the experiment, Julian dates 81-83, and receiver S3, which was located 400 m away from the transmitter. We will consider 8-QAM, 16-QAM, and two MIMO setups: one with two transmitters and one with three transmitters. These setups have been studied in [12] with the turbo-equalization receiver.

The performance results with $N_t = 2$ are plotted in Fig. 4, where we combine an increasing number of hydrophones to illustrate the performance differences. Generally an iterative receiver can gain significantly over a non-iterative receiver. For 8-QAM in Fig. 4, we find that thresholded soft feedback performs the best, followed by hard feedback where channel estimation is updated only every other iteration (denoted as $\times 2$). For 16-QAM in Fig. 4, full soft or hard feedback (where channel estimation is updated every iteration, denoted as $\times 1$) performs the best.

The performance results with $N_t = 3$ are plotted in Fig. 5. We see similar trends: the iterative receiver gains significantly over the non-iterative receiver; for 8-QAM thresholded soft feedback and hard feedback ($\times 2$) slightly outperform the

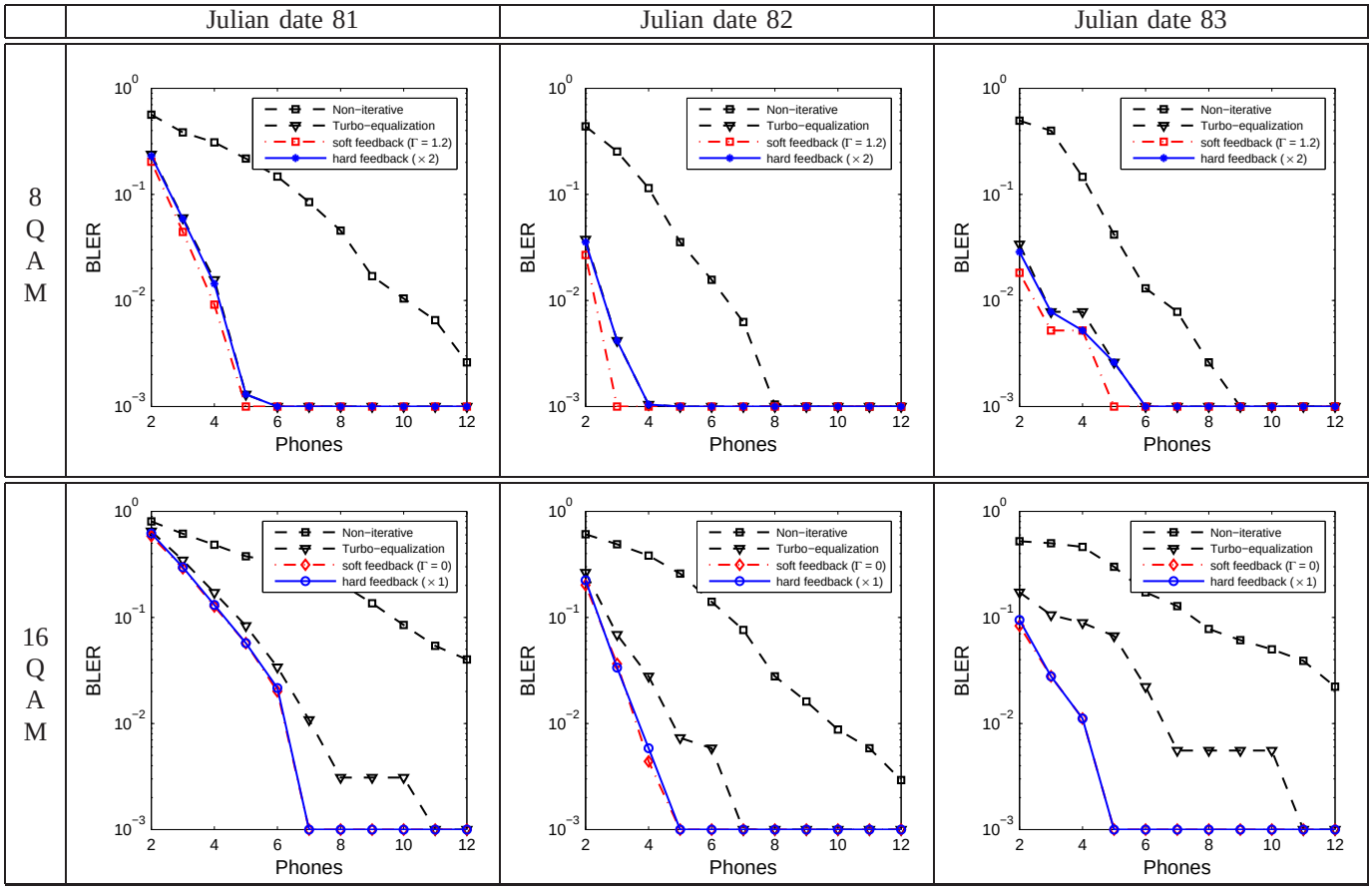

Fig. 4. Experimental results from the RACE08 experiment on MIMO-OFDM with $N_t = 2$.

TABLE I

PERFORMANCE RESULTS WITH HIGH DATA RATES FROM RACE08; TWELVE RECEIVERS USED.

	Spectral efficiency	Data streams	Average BER	Average BLER
3IMO, 64-QAM	5.28 bits/s/Hz	Stream 1	$2.8 \cdot 10^{-1}$	$9.9 \cdot 10^{-1}$
		Stream 2	$6.0 \cdot 10^{-2}$	$1.8 \cdot 10^{-1}$
		Stream 3	$9.1 \cdot 10^{-2}$	$2.7 \cdot 10^{-1}$
4IMO, 16-QAM	4.69 bits/s/Hz	Stream 1	$9.4 \cdot 10^{-2}$	$4.5 \cdot 10^{-1}$
		Stream 2	$2.8 \cdot 10^{-2}$	$9.0 \cdot 10^{-2}$
		Stream 3	$2.7 \cdot 10^{-2}$	$8.3 \cdot 10^{-2}$
		Stream 4	$1.6 \cdot 10^{-2}$	$5.6 \cdot 10^{-2}$

turbo-equalization receiver; and for 16-QAM full soft or hard feedback give a sizable gain over turbo-equalization.

In Table I, we also include results for two setups not studied in [12]: (i) $N_t = 3$, 64-QAM and (ii) $N_t = 4$, 16-QAM, having spectral efficiencies of 5.28 and 4.69 bits/s/Hz, respectively. The results are based on Julian date 83 only, and $N_r = 12$ receive-elements are used. Although data stream one performs poorly due to the transducer issue (see discussion in [12]), the other data streams can be decoded at reasonable levels.

VI. EXPERIMENTAL RESULTS: SPACE08

The SPACE08 experiment was held off the coast of Martha's Vineyard, MA, from Oct. 14 to Nov. 1, 2008. The water depth was about 15 meters. The system parameters are the same as in the numerical simulation section.

We focus on receivers S3 and S5 that were located 200 m and 1,000 m from the transmitter, respectively. We use data from three days: Julian dates 297-299. Due to the more challenging environment, we will only consider the small-size QPSK constellation. The data rate for a $N_t = 2$ or $N_t = 3$ MIMO system using QPSK modulation is 10.4 and 15.6 kb/s respectively. Performance results are plotted in Fig. 6 for $N_t = 2$ and in Fig. 7 for $N_t = 3$. For QPSK modulation we do not see any significant improvement using thresholding as all symbols are of unit energy. We therefore plot full soft and hard feedback only. For $N_t = 2$, we observe a sizable gain using updated channel estimates, while

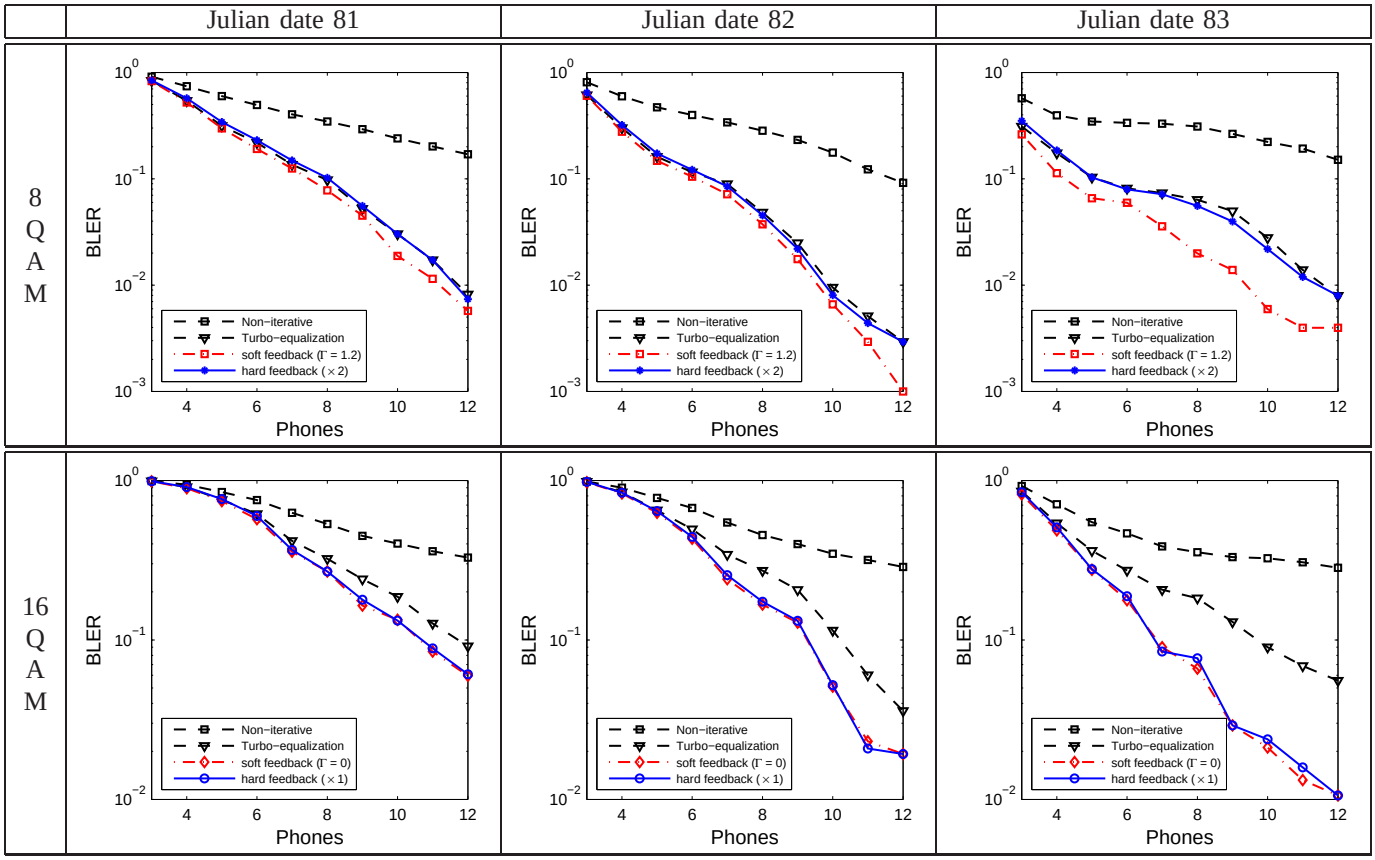

Fig. 5. Experimental results from the RACE08 experiment on MIMO-OFDM with $N_t = 3$.

all iterative receivers gain significantly over the non-iterative receiver. For the $N_t = 3$ setup, the gain of updated channel estimates is more pronounced. This seems reasonable, as less pilots are available for channel estimation per transmitter in this case.

VII. Conclusion

In this paper, we developed an iterative receiver for underwater MIMO-OFDM that couples sparse channel estimation, MIMO detection, and channel decoding. Various types of feedback information were considered to improve the sparse channel estimator using the Basis Pursuit algorithm. We tested the proposed receiver extensively using numerical simulation and experimental data. All iterative receivers gain significantly over a non-iterative receiver.

Depending on the constellation, different feedback strategies could perform differently. Specifically, for 8-QAM, reducing the number of erroneous feedback by using soft-thresholding or performing repeated MIMO demodulation before updating channel estimates performs best, while For 16-QAM, full soft or hard feedback performs best. Further investigation is needed to understand how various feedback strategies affect the system performance.

References

[1] D. B. Kilfoyle, J. C. Preisig, and A. B. Baggeroer, "Spatial modulation experiments in the underwater acoustic channel," *IEEE J. Ocean. Eng.*, vol. 30, no. 2, pp. 406–415, Apr. 2005.

[2] H. C. Song, P. Roux, W. S. Hodgkiss, W. A. Kuperman, T. Akal, and M. Stevenson, "Multiple-input/multiple-output coherent time reversal communications in a shallow water acoustic channel," *IEEE J. Ocean. Eng.*, vol. 31, no. 1, pp. 170–178, Jan. 2006.

[3] S. Roy, T. M. Duman, V. McDonald, and J. G. Proakis, "High rate communication for underwater acoustic channels using multiple transmitters and space-time coding: Receiver structures and experimental results," *IEEE J. Ocean. Eng.*, vol. 32, no. 3, pp. 663–688, Jul. 2007.

[4] J. Tao, Y. R. Zheng, C. Xiao, T. C. Yang, and W.-B. Yang, "Time-domain receiver design for MIMO underwater acoustic communications," in *Proc. of MTS/IEEE OCEANS Conf.*, Quèbec City, Quèbec, Sept. 2008.

[5] J. Zhang, Y. R. Zheng, and C. Xiao, "Frequency-domain equalization for single carrier MIMO underwater acoustic communications," in *Proc. of MTS/IEEE OCEANS Conf.*, Quèbec City, Quèbec, Sept. 2008.

[6] F. Qu and L. Yang, "Basis expansion model for underwater acoustic channels?" in *Proc. of MTS/IEEE OCEANS Conf.*, Quèbec City, Quèbec, Sept. 2008.

[7] A. Song, M. Badiey, and V. K. McDonald, "Multi-channel combining and equalization for underwater acoustic MIMO channels," in *Proc. of MTS/IEEE OCEANS Conf.*, Quèbec City, Quèbec, Sept. 2008.

[8] J. Ling, T. Yardibi, X. Su, H. He, and J. Li, "Enhanced channel estimation and symbol detection for high speed MIMO underwater acoustic communications," in *Proc. of the 2009 DSP & SPE Workshop*, Marco Island, FL, Jan. 2009.

[9] J. Zhang, Y. R. Zheng, and C. Xiao, "Frequency-domain turbo equalization for MIMO underwater acoustic communications," in *Proc. of MTS/IEEE OCEANS Conf.*, Bremen, Germany, May 2009.

[10] B. Li, S. Zhou, M. Stojanovic, L. Freitag, J. Huang, and P. Willett,

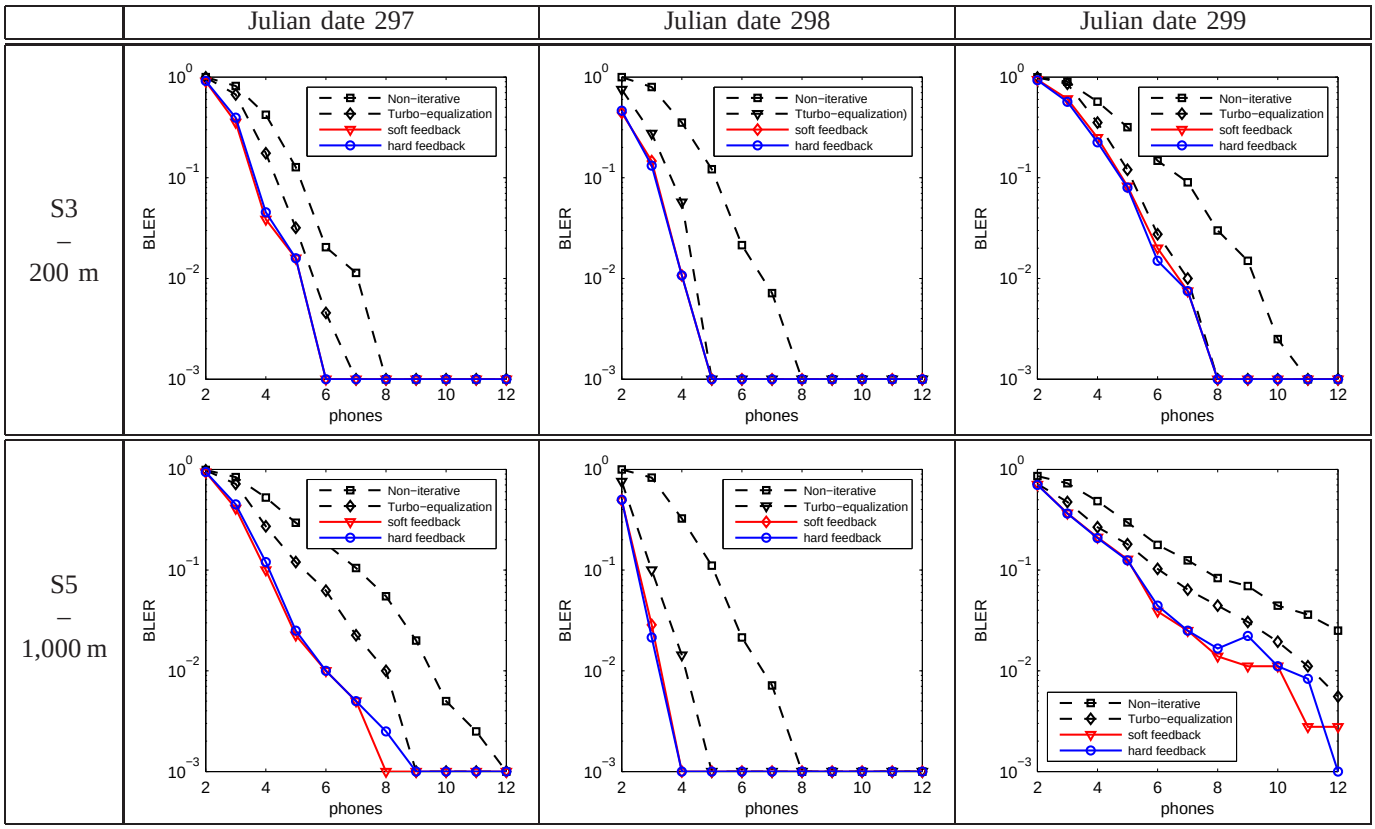

Fig. 6. Experimental results from the SPACE08 experiment on MIMO-OFDM with $N_t = 2$, QPSK, for S3 (200 m) and S5 (1,000 m).

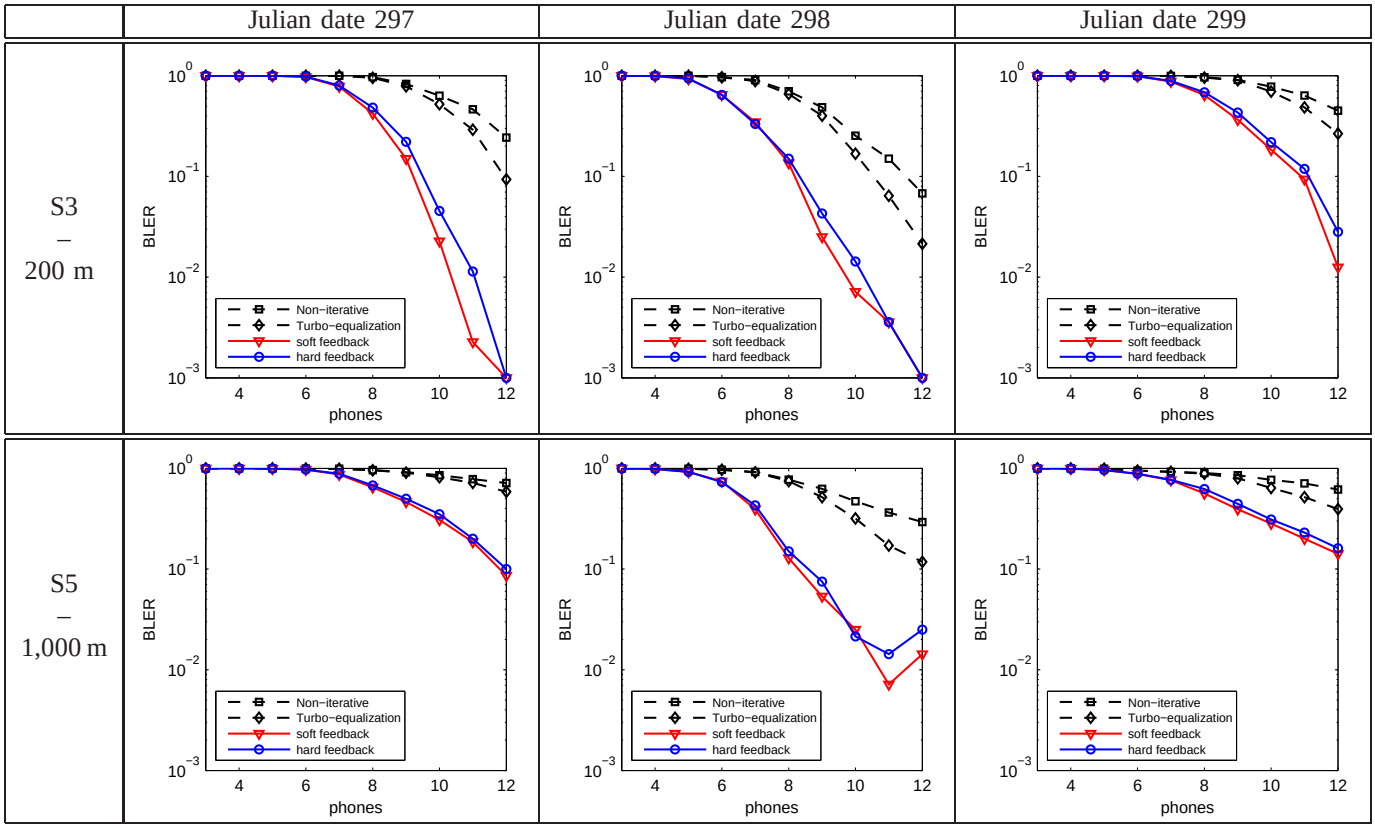

Fig. 7. Experimental results from the SPACE08 experiment on MIMO-OFDM with $N_t = 3$, QPSK, for S3 (200 m) and S5 (1,000 m).

"MIMO-OFDM over an underwater acoustic channel," in *Proc. of MTS/IEEE OCEANS Conf.*, Vancouver, BC, Canada, 2007.

[11] Y. Emre, V. Kandasamy, T. M. Duman, P. Hursky, and S. Roy, "Multi-input multi-output OFDM for shallow-water UWA communications," in *Proc. of ACOUSTICS 2008*, Paris, France, 2008.

[12] B. Li, J. Huang, S. Zhou, K. Ball, M. Stojanovic, L. Freitag, and P. Willett, "Further results on high-rate MIMO-OFDM underwater acoustic communications," in *Proc. of MTS/IEEE OCEANS Conf.*, Quèbec City, Quèbec, Sept. 2008.

[13] P. Carrascosa and M. Stojanovic, "Adaptive MIMO detection of OFDM signals in an underwater acoustic channel," in *Proc. of MTS/IEEE OCEANS Conf.*, Quèbec City, Quèbec, Sept. 2008.

[14] M. Stojanovic, "Adaptive channel estimation for underwater acoustic MIMO OFDM systems," in *Proc. of IEEE DSP Workshop*, Marco Island, FL, Jan. 2009.

[15] F. Qu and L. Yang, "Rate and reliability oriented underwater acoustic communication schemes," in *Proc. of the 2009 DSP & SPE Workshop*, Marco Island, FL, Jan. 2009.

[16] C. R. Berger, S. Zhou, J. Preisig, and P. Willett, "Sparse channel estimation for multicarrier underwater acoustic communication: From subspace methods to compressed sensing," in *Proc. of MTS/IEEE OCEANS Conf.*, Bremen, Germany, May 2009.

[17] S. Mason, C. R. Berger, S. Zhou, K. Ball, L. Freitag, and P. Willett, "An OFDM design for underwater acoustic channels with Doppler spread," in *Proc. of the 2009 DSP & SPE Workshop*, Marco Island, FL, Jan. 2009.

[18] M. C. Valenti and B. D. Woemer, "Iterative channel estimation and decoding of pilot symbol assisted Turbo codes over flat-fading channels," *IEEE J. Select. Areas Commun.*, vol. 19, no. 9, pp. 1697–1705, Sept. 2001.

[19] H. Niu and J. A. Ritcey, "Iterative channel estimation and decoding of pilot symbol assisted LDPC coded QAM over flat fading channels," in *Proc. of Asilomar Conf. on Signals, Systems, and Computers*, vol. 1, Pacific Grove, CA, Nov. 2002, pp. 2265–2269.

[20] H. Niu, M. Shen, J. A. Ritcey, and H. Liu, "A factor graph approach to iterative channel estimation and LDPC decoding over fading channels," *IEEE Trans. Wireless Commun.*, vol. 4, no. 4, pp. 1345–1350, Jul. 2005.

[21] J. Wu, B. Vojcic, and Z. Wang, "Cross-entropy based symbol selection and partial iterative decoding for serial concatenated convolutional codes," in *Proc. of Conf. on Information Sciences and Systems (CISS)*, Princeton, NJ, Mar. 2008.

[22] T. Kang and R. A. Iltis, "Iterative carrier frequency offset and channel estimation for underwater acoustic OFDM systems," *IEEE J. Select. Areas Commun.*, vol. 26, no. 9, pp. 1650–1661, Dec. 2008.

[23] J. Huang, S. Zhou, and P. Willett, "Nonbinary LDPC coding for multicarrier underwater acoustic communication," *IEEE J. Select. Areas Commun.*, vol. 26, no. 9, pp. 1684–1696, Dec. 2008.

[24] B. Li, S. Zhou, M. Stojanovic, L. Freitag, and P. Willett, "Multicarrier communication over underwater acoustic channels with nonuniform Doppler shifts," *IEEE J. Ocean. Eng.*, vol. 33, no. 2, Apr. 2008.

[25] D. Donoho, "Compressed sensing," *IEEE Trans. Inform. Theory*, vol. 52, no. 4, pp. 1289–1306, Apr. 2006.

[26] S.-J. Kim, K. Koh, M. Lustig, S. Boyd, and D. Gorinevsky, "An interior-point method for large-scale l_1-regularized least squares," *IEEE J. Select. Topics Signal Proc.*, vol. 1, no. 4, pp. 606–617, Dec. 2007.